CHAPTER

InAs/InP quantum-dash lasers

5

M.Z.M. Khan[a], E.A. Alkhazraji[a], M.T.A. Khan[a], T.K. Ng[b], B.S. Ooi[b]

[a]Optoelectronics Research Laboratory, Electrical Engineering Department, King Fahd University of Petroleum & Minerals, Dhahran, Saudi Arabia; [b]Photonics Laboratory, Computer, Electrical and Mathematical Sciences and Engineering (CEMSE) division, King Abdullah University of Science & Technology (KAUST), Thuwal, Saudi Arabia

1. Introduction

With the advent of the optical fiber technology, the ever-increasing demand for wide bandwidth reliable solutions to satiate the today's world's thirst for in the 1.55 μm C-band optical communication window has driven analysis and research for high performance active optical devices including light-emitting diodes, semiconductor lasers, semiconductor optical amplifiers (SOA), mode-locked lasers, and modulators. Quantum confined nanostructure based active-regions in the form of quantum-wells (Qwells) and self-assembled quantum-dots (Qdots) have been garnering the focus of research in the past couple of decades as prime contenders for the sought highly efficient compact semiconductor devices and optical sources owning to the high quality epitaxial growth on GaAs substrates emitting at ~1.3 μm and being commercialized with excellent performance parameters. Nevertheless, their inability to reach the C-band window of 1.55 μm and beyond resulted in InP substrate-grown devices to take spot light of research and to commercially dominate over their GaAs counterparts [1,2].

However, a new class of self-assembled nanostructures, dubbed as quantum dash, has emerged as elongated quantum wire-like structures resulting from the small lattice mismatch during self-assembly growth of Qdots. These Qdashes exhibit peculiar characteristics in-between Qwell and Qdots and have shown to exhibit a wide tuning range of emission from ~1.5 μm and all the way up to ~2.0 μm and beyond [3–5]. These InAs nanostructures on both InGaAlAs and InGaAsP material systems alike have witnessed wide strides in research and development while displaying decent performance parameters. Nevertheless, the inherent inhomogeneous nature of these structures in the form of their shape and size dispersion as a result of the self-assembled growth process itself poses and obstacle in realizing high quality epitaxial material and, thus the results laser device performance.

With that said, the very inhomogeneous nature of InAs/InP Qdashes can be rather exploited for their ultra-broad gain profiles and utilized as broadband laser components with coverage bandwidths exceeding 50 nm [6]. Furthermore, with passive

Nanoscale Semiconductor Lasers. https://doi.org/10.1016/B978-0-12-814162-5.00005-4

mode-locking, ultra-short femto-second pulse trains can be generated which can be crucial in applications including wavelength-division multiplexed (WDM) optical communication systems and high-speed optical time-domain multiplexers (OTDMs). Moreover, the remarkable tunability that has been shown by these structures covering the entire C−, L−, and U−optical communication bands and even exceeding 2 μm, in addition to the aforementioned ultra-broad gain profiles can be invaluable to serve multi-disciplinary applications. In medical applications, for once, InAs/InP Qdash based lasers offer low cost compact solution with a high tunability and axial resolution to potentially replace bulk and solid state lasers in medical diagnosis, optical coherent tomography, bio-molecular and tissue imaging, and high-precision surgery and dentistry [7−11]. Nonetheless, in molecular and material sensing and characterization, these devices can be utilized as portable broad long wavelength sources in applications such as light detection and ranging (LIDAR), chemical sensing, in-situ multicomponent analysis, and spectroscopy. Furthermore, the exceptionally broad spectra of such optical laser sources can be very beneficial to some fields such as non-destructive testing, material research, imaging ceramics, birefringence imaging of crystalline polymer structures and studying their penetration depths [12].

In this chapter, we discuss the existing self-assembled growth of InAs Qdash based nanostructures on (100) and (311) B InP substrates for eventual operation in the C − L − U band and toward 2 μm. The tremendous progress in this area resulted in an astounding amount of literature. Section 2 of this chapter discusses the achievements in the epitaxial material growth of InAs/InP quantum dash material systems. Subsequently, Section 3 discusses the device-level employment of these structures as semiconductor laser sources in addition to the respective utilization of optical injection (injection locking) and mode-locking in their employment. Finally, Section 4 concludes this chapter by discussing the recent employment of Qdash lasers as promising sources for future optical communication systems.

2. Growth of InAs/InP quantum dash lasers

The phrase “Quantum dash” was introduced at the end of the last century with the first introduction of self-assembled InAs Qdashes grown over (211)B GaAs substrates by Guo et al. [12] and InSb Qdashes over (100) InP substrates by Utzmeier et al. [13]. However, only at the beginning of this millennium is when they properly began being employed and identified in actual optoelectronic applications. Qdash laser structures were dominated by two material systems: (i) InAs/InGaAlAs and (ii) InAs/InGaAsP.

2.1 InAs/InGaAlAs material system

In 1999, via Molecular Beam Epitaxy (MBE), Li et al. [14] introduced a 6-stack of high density ($\sim 70\ \mu m^{-1}$) InAs/$Al_{0.48}In_{0.52}As$ quantum-wire like nanostructures, on

a (100) InP substrate with InAlAs buffer layers. The structure displayed a photoluminescence (PL) peak at 1.9 μm in addition to a large anisotropy that was scribed to results in the reported high density. Later on, through TEM analysis, they concluded that increasing the deposition of InAs from 1.5 to 7.5 monolayer (ML) resulted in increasing the inhomogeneity and the sizes of the formed Qdashes [15].

The first report of dash-in-well (DaWELL) structure was by Wang et al. [3] who demonstrated the growth of InAs Qdashes with a density of $\sim 10^{10}$ cm^{-2} within an asymmetric InGaAlAs Qwell layer separated by strained barrier layers of InGaAlAs that exhibited a PL peak at $\sim$1.57 μm. To follow up, a parametric study was carried out by Schwertberger et al. [16] on different MBE Qdash InAs growth parameters. It was observed that at a fixed substrate temperature, increasing the thickness of the deposited InAs from 2.5 to 7 ML had dramatically increased the height and decreased the length of the Qdashes. Fig. 5.1A shows the PL spectra at different nominal InAs layer thickness covering the emission band from $\sim$ 1.2 to $\sim$ 2.0 μm. Nevertheless, more deposition thickness was found to lead the Qdashes to coalesce into islands of greater size with a reduction in the dash nature of the structure. Moreover, the substrate growth temperature was investigated after which they suggested an optimal value of $\sim$500 °C that was observed to result in a maximum PL intensity.

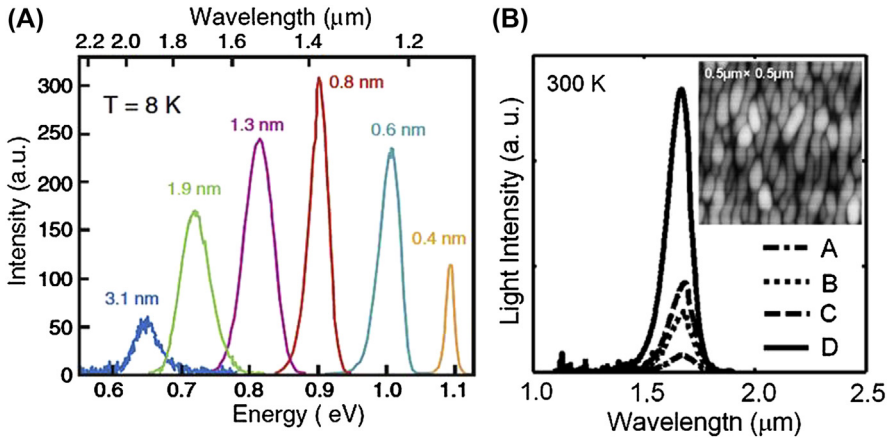

FIG. 5.1

(A) Low temperature PL spectra of Qdash layers with different nominal InAs layer thickness as indicated in the figure, on InGaAlAs buffer layer on (100) InP substrate [16]. (B) PL spectra measured at 300 K for four InAs Qdash samples grown at various conditions (A and B with InGaAlAs barrier grown at 505 °C and 535 °C, respectively. C and D are similar to B except an ultra-thin GaAs layer was grown before the growth of InAs layer, and before and after the growth of InAs layer, respectively). Inset shows the (0.5×0.5 μm^2) AFM image of an InAs Qdash layer without InAlGaAs cap [19].

From Khan MZM, Ng TK, Ooi BS. Self-assembled InAs/InP quantum dots and quantum dashes: material structures and devices. Progress in Quantum Electronics 2014;38(6):237–313.

Rotter et al. reported another striking tunability of DaWELL structure [17] as then demonstrated a PL peak emission shift between 1.52 and 2.04 μm. Later, Sauerwald et al. [18] showed that the emission of a single stack of Qdash can be tuned in the range of 1.39−1.90 μm undependably of the composition and the shape of the Qdashes by adjusting the thickness of InAs deposition which they demonstrated to have a linear relationship with the size of the grown Qdashes leading to red shifting the PL peak in addition to broadening its linewidth. Moreover, they extended the investigation [19] to cover multistacks of InAs/InGaAlAs DaWELL structures to analyze the effect of more Qdash layer stacking which was shown to increase the size of the grown Qdashes. This was attributed to the extra strain effects in the upper layers that resulted in the merging of the grown dashes at different rates which ultimately results in more inhomogeneity in the DaWELL structure.

Later, Mi et al. [20] demonstrated the possibility of achieving a significantly better optical performance by growing ultrathin layers (∼2 ML) of GaAs over the InGaAlAs barrier prior to deposing InAs. As such, they reported more than 3 times higher PL intensity as depicted in Fig. 5.1B while a more drastic enhancement (>10 times) in the PL intensity along with a reduced linewidth (∼50 meV) is achieved when more GaAs layers are deposited after the growth of the capping layer which all was accredited to the suppressed phase separation and enhanced surface migration in the barrier layer. In 2008, Podemski et al. [21] reported a highly stacked columnar Qdashes over (100) InP that are sandwiched between InGaAlAs layers and within buffer layers of InAlAs. They demonstrated that the dominant polarization could be transitioned from transverse electric to transverse magnetic via controlling the number of stacking layers from 1 to 24 in addition to red shifting the PL peak, as shown in Fig. 5.1D due to the larger sizes of the grown Qdashes.

2.2 InAs/InGaAsP material system

González et al. [22] demonstrated the significance of the buffer layer in forming InAs nanostructures by growing buffer layer of InP using atomic-layer MBE that yielded in self-assembled quantum wire-like structures that are elongated in the [1−10] direction. Then, it was postulated that anisotropic stress relaxation of the heteroepitaxial system involving different group V elements was responsible in the formation of these Qwires [23]. Later, Gendry et al. showed [24] that increasing the growth temperature results in lowering the critical thickness of the growth mode transition of a single stack of quantum-sticks within a matrix layer of InP. This in turn, leads to reducing the height dispersion of the grown dashes making for a more uniform grown island as illustrated in Fig. 5.2A. Furthermore, it was found that few growth parameters can be optimized to reduce the height dispersion including reducing the Arsenic overpressure during InAs deposition (as shown in Fig. 5.2B), increasing the InAs thickness drastically, and higher growth temperature. This was attributed to the thermodynamics and kinetics such as adatom surface diffusion and strain accumulation which improved the self-organization of the grown islands [24]. Building upon that work, Fuster et al. [25] investigated the effect

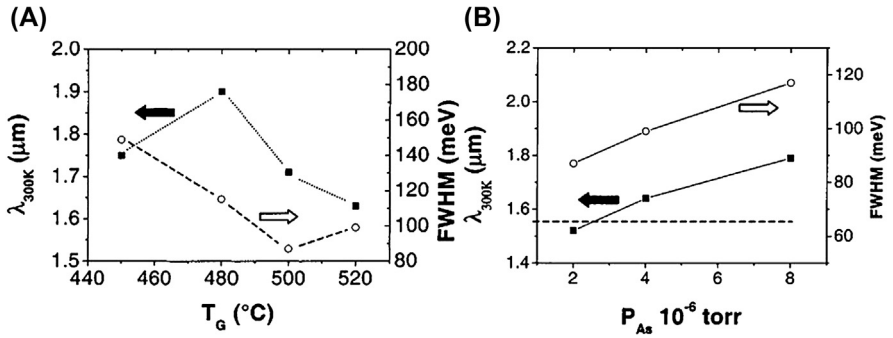

FIG. 5.2

(A) PL characteristics [peak emission and linewidth] of InAs island's PL spectra on InP buffer layer at 300 K as a function of the growth temperature for an InAs deposition thickness just above (∼0.5 ML) the critical thickness. (B) PL characteristics of InAs islands on InP at 300 K versus the As overpressure during the InAs growth (growth temperature 520 °C, InAs deposition thickness 0.9 nm) [24].

From Khan MZM, Ng TK, Ooi BS. Self-assembled InAs/InP quantum dots and quantum dashes: material structures and devices. Progress in Quantum Electronics 2014;38(6):237–313.

of thickness of the InAs layer which was found to have a proportional relationship with the size of the formed Qwires, as illustrated in Fig. 5.3A, which lies in line with the other reports on the InAs/InGaAlAs material system.

Subsequently, Alen et al. [26] showed that structures of thinner InP spacer layers were associated with a higher degree of homogeneity by comparing two specimens of 10-stack InAs/InP Qwires grown over spacer layers of 5 and 10 nm. This uniformity was accredited to the strain driven vertical filtering of the size of the grown Qwires along growth direction. On the other hand, thicker spacer layers resulted in high inhomogeneity with a broad PL linewidth of ∼350 meV which agrees with Podemski et al. [21] work on the InAs/InGaAlAs material system. Later, Lelarge et al. empirically utilized [27] growth conditions, number of layers Qdashes, their thickness, and the strain of the barrier layers as parameters in order to identify the nominal thickness of subsequent layers that compensated for any thickening of the Qdashes during growth which ultimately enabled achieving homogeneity in the sizes of the Qdashes without ultrathin barrier layers. As such, they demonstrated up to 10 stacks with a barrier layer thickness of 40 nm with a minimal impact on the PL linewidth as it was kept around ∼70 meV, as shown in Fig. 5.3B. Keeping up with the same purpose, Faugeron et al. [28] introduced an alternative methodology. They adopted an asymmetrical cladding technique by inserting an undoped index slab layer between the Qdash active region and the substrate. This introduction resulted in a reduced overlap among the optical modes which maintained the PL linewidth and optical quality of the 6-stach structure whose PL peak at ∼1.57 μm.

On other front, several works have been carried to increase the Qdash structure inhomogeneity. Although, this inherently demerits the optical performance of Qdash

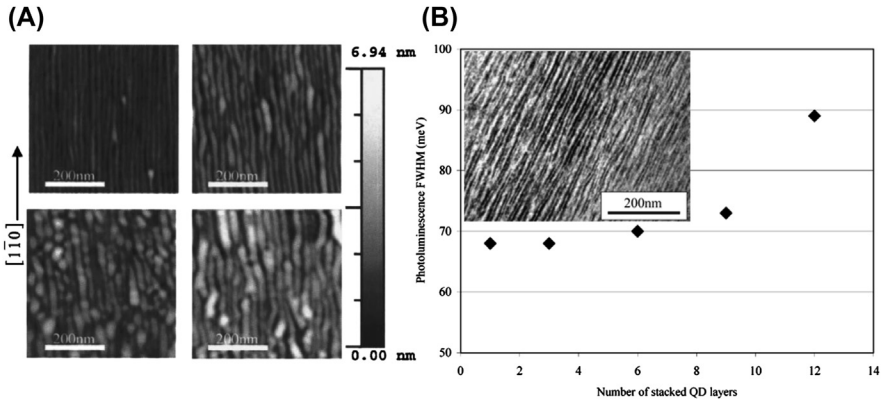

FIG. 5.3

(A) AFM images ($0.5 \times 0.5\ \mu m^2$) of four uncapped InAs Qwire samples with different InAs deposited thicknesses 2.5 ML, 3.3 ML, 4.3 ML, and 5.3 ML from upper left to bottom right. The four images have the same z-scale bar [25]. (B) Room temperature PL linewidth of stacked InAs/InGaAsP Qdashes as a function of the number of stacking layers. Inset shows the plan-view TEM micrograph of a stack of 6 Qdash layers [27].

From Khan MZM, Ng TK, Ooi BS. Self-assembled InAs/InP quantum dots and quantum dashes: material structures and devices. Progress in Quantum Electronics 2014;38(6):237–313.

lasers due to the trade-off between the spectral linewidth and threshold gain, in some applications such as WDM based communications and realization of semiconductor optical amplifier (SOA), the need for the inhomogeneous broadening warrants said trade-off. With that goal in sight, Deubert et al. [29] introduced a chirping technique where the InAs nominal thicknesses a 6-stack Qdash structure was varied between 3 and 4.6 ML at a fixed barrier thickness of 25 nm. This yielded in a broad PL that was ~45% higher to the traditional 4-stack structure with a fixed InAs layer thickness. Soon after, Reithmaier et al. [30] reported a large gain-bandwidth of 270 nm with peak gain of 40 cm^{-1} using a similar chirped design of 4 varying InAs layers at a fixed barrier layer. Based on the analytical results of the thickness of the barrier layer on the inhomogeneity of the structure [31], our group demonstrated [32] an ultrabroad PL linewidth of ~151 nm by utilizing a chirped 4-stack InGaAlAs DaWELL structure with varying barrier layers (20, 15, 10, 10 nm) that was drastically broader than a similar structure of a fixed barrier layer thickness (10 nm) among the different layers where the PL linewidth was ~100 nm. Under continuous wave (CW) current density of 8.3 kA/cm^2, the gain-bandwidth was measured [33] as ~140 nm with a peak modal gain of ~41 cm^{-1} as shown in Fig. 5.4A.

Very recently, Pes et al. utilized Gas Source MBE in growing a 6-stack InAs Qdashes of 3 sets on a (001) InP substrate [34]. Each Qdash layer was separated by a $In_{0.8}Ga_{0.2}As_{0.435}P$ barrier layer of a thickness of 15-nm and surrounded by quaternary alloy layers whose thickness was chosen to ensure a homogenous excitation

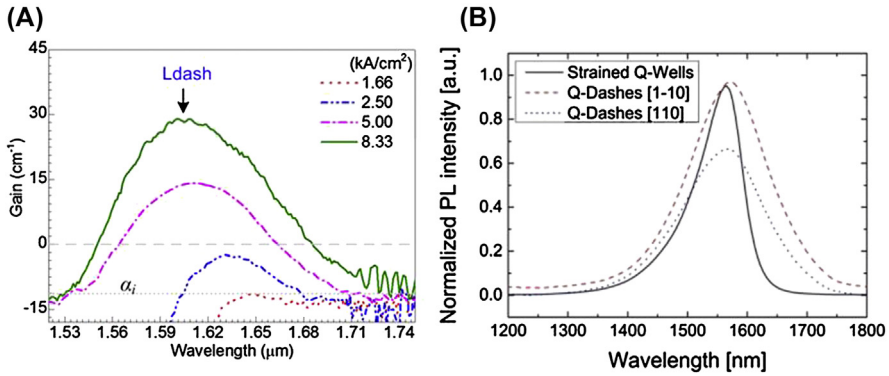

FIG. 5.4

(A) Gain of a four stack DaWELL InAs/InGaAlAs/InP laser structure with chirped barrier layer thickness (10, 10, 15, 20 nm) [33]. (B) PL spectra of two specimens of 6-stack InAs Qdashes along two different directions compared to a strained quantum-well structure.

From Khan MZM, Ng TK, Ooi BS. Self-assembled InAs/InP quantum dots and quantum dashes: material structures and devices. Progress in Quantum Electronics 2014;38(6):237–313. Also reprinted with permission from Pes S, et al. Class-A operation of an optically-pumped 1.6 μm-emitting quantum dash-based vertical-external-cavity surface-emitting laser on InP. Optical Express 2017;25(10):11760–6.

of the active region. The PL of two Qdash specimens elongated along the [1−10] and [110] directions, as shown in Fig. 5.4B, showed a very broad linewidth while keeping the integrated PL intensity comparable to that of a 6-stack strained quantum-well structure, thus providing more insight to Qdash active region physics.

3. InAs/InP Qdash lasers

In this section, we discuss Qdash active regions in edge-emitting Fabry-Perot lasers, injection-locked lasers, and mode-locked lasers. Owning to the inhomogeneous nature of their structure, the stimulated emission of Qdash lasers is associated with broad spectral linewidth as has been discussed earlier. In addition, the resulted sub-picosecond pulses with mode locking has the potential to improve the performance dramatically.

3.1 InAs/InGaAlAs/InP Qdash lasers

Wang et al. were first to demonstrate a semiconductor Qdash [3] active region based laser that consisted of 1−, 3−, and 5−stack InAs/InGaAlAs DaWELL and emitting at 1.60, 1.62, and 1.66 μm, respectively. Fig. 5.5A shows the L-I characteristics while the electroluminescence spectrum is shown in its inset. The devices were 1.5−4.0 mm long broad-area lasers with threshold current densities of 410, 167, and 766 A/cm^2 per layer, respectively, while the internal loss and internal quantum

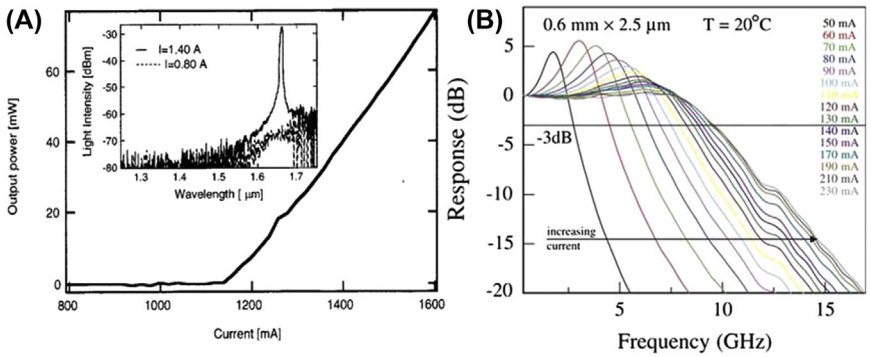

FIG. 5.5

(A) A two-facet light output versus pulsed injection current measured on a five-stack Qdash laser diode with geometry of 100 × 1500 μm^2 [3]. The inset in (A) is the electroluminescence spectra under different pump levels for the device [38]. (B) Room temperature small-signal modulation response of a ridge-waveguide 2.5 × 600 μm^2 undoped InAs/InGaAlAs Qdash laser for various CW drive currents [42].

From Khan MZM, Ng TK, Ooi BS. Self-assembled InAs/InP quantum dots and quantum dashes: material structures and devices. Progress in Quantum Electronics 2014;38(6):237–313.

efficiency were $\sim$10 cm^{-1} and $\sim$60%, respectively. These promising results in addition to the $\sim$15 cm^{-1} acquired modal gain, were bound to motivate and push research and further investigation on this particular system. As such, Schwertberger et al. [35] later demonstrated the tunability of InAs/InGaAlAs Qdash lasers in the range of 1.54–1.78 μm by tuning the thickness of InAs deposition layer between 5.0 and 7.5 ML. A low threshold current density of 225 A/cm^2 per layer off a 4-stack 40 × 1000 μm^2 device was reported, with total output power exceeding 100 mW and a characteristic temperature T_0 of $\sim$61 K. Later on, with an improved material quality evident by the 60% quantum efficiency and 8.5 cm^{-1} internal loss [16], the transparency current density was further reduced to as low as 90 A/cm^2 per layer which is one of the best values reported on this material system. On the same venue, Rotter et al. [17] were able to push the emission wavelength to as long as 2.03 μm which is the longest emission wavelength reported on any InAs/InP Qdash laser structure. This was carried out on a 5-stack InAs DaWELL structure over a (100) InP substrate with a 52% internal quantum efficiency and a per-layer threshold current density of 108 A/cm^2. However, the significantly high internal loss of $\sim$55 cm^{-1} was attributed to Rayleigh scattering that was caused by the refractive index local undulations in the vicinity of the Qdashes.

Subsequently, Resneau et al. [36] demonstrated a flat low relative intensity noise (RIN) of −162 dB/Hz and a total power >100 mW on a 4 stack graded separate confinement heterostructure (SCH) InAs/InGaAlAs ridge-waveguide Qdash laser emitting at 1.57 μm. Furthermore, the corresponding internal loss was very low 4 cm^{-1} which is among the lowest on this material system. Furthermore, through

the dynamic characteristics measurements, the acquired modulation efficiency and maximum intrinsic bandwidth were of 0.36 GHz/mA$^{0.5}$ and 5.9 GHz, respectively, while the K-factor was 1.51 ns. Later on, the modulation efficiency and resonance frequency were pushed to 0.72 GHz/mA$^{0.5}$ and 7.5 GHz, respectively [37]. On another front, Mi et al. [20] demonstrated the largest small signal modulation bandwidth (up to 12 GHz) in an InAs/InP Qdash system at any temperature (°C) with a reduced sub-threshold linewidth-enhancement factor (LEF) <0.7 and a high characteristic temperature T_0 of ~204 K. This was attributed to the minimized carrier leakage and hot carrier effects by the virtue of the p-doping and tunnel injection that were implemented simultaneously. Nevertheless, the best small signal modulation bandwidth in a Qdash system at room temperature was 9.6 GHz that was reported by Hein et al. [38] who employed a 2.5 × 600 μm^2 undoped 6-stack InAs/InGaAlAs Qdash laser under CW operation. The obtained modulation efficiency was 0.82 GHz/mA$^{0.5}$ while the K-factor and maximum intrinsic bandwidth were 0.78 ns and 11.4 GHz, respectively as depicted in Fig. 5.5B. Moreover, the above-threshold LEF was acquired as 2.5 via the amplitude-modulation/frequency-modulation method. In terms of the threshold current density, Hein et al. [39] reported the best value in any multi-stack Qdash (46 A/cm^2 per layer) system and on a 16-stack 1.3-mm long columnar Qdash laser structure that lased at 1.7 μm, followed by 108 A/cm^2 per layer threshold current density value reported by Rotter et al. [17]. On the other hand, the 93% internal quantum efficiency of the 4-stack Qdash laser that was reported by our group [40] is the highest in a Qdash laser. Furthermore, our group also demonstrated the enhancement in the performance of the Qdash laser lasing at ~1.61 μm in the form of a ~45% and ~11% reduction in the transparency current density and threshold current, respectively without compromising the other laser performance parameters via controlling the IFVD intermixing process.

Very recently, Rudno-Rudziński et al. [41] investigated the influence of the width of the quantum well layer on the injection-tunneling of Qdash based material system. The InAs Qdashes were separated from the InGaAs quantum-well layer by a 2.3-nm thick barrier layer. The coupling affects both spectral and temporal optical response by altering the isolated 0D character of the ground state emission for wide quantum wells. In such cases, it was suggested that the ground state emission becomes indirect, as evident by the elongation of the PL decay time from 2 ns to 10 ns.

3.2 InAs/InGaAsP/InP Qdash lasers

This material system was adopted relatively later in Qdash lasers starting with Moreau et al.'s [42] report on the effects of p-doping and multi-stacking on the performance of a 9-stack InAs/InGaAsP DaWELL laser on (100) InP substrate emitting at 1.52 μm. A low threshold current density of 123 A/cm^2 per layer was obtained from the 50 × 600 μm^2 device at room temperature. In addition, the transparency current density was found as 83 A/cm^2 per layer while the modal gain was 5.4 cm^{-1} per

layer. The results were found to be superior when in comparison with the performance of a 6-stack and 12-stack Qdash lasers.

In a different report, Lelarge et al. [27] demonstrated a significant improvement in the transparency current density of a 50 × 2000 μm^2 DaWELL laser [660 A/cm^2 (110 A/cm^2 per layer)] when compared with a similar Qdash-in-barrier based laser [1140 A/cm^2 (190 A/cm^2 per layer)], likely due to the better carrier injection [43] in the case of the former scheme, as shown in Fig. 5.6A. Moreover, this was accompanied by redshift in the emission from 1.56 to 1.65 μm in the former and latter schemes, respectively. The internal loss and internal quantum efficiency were obtained as 19 cm^{-1} and 80% while the modal gain was high 105 cm^{-1}. It was also pointed out that despite of the p-doping, the characteristic temperature T_0 ~60 K did not exhibit a significant increase possibly due to either the band structure or the shape of the nanostructures. Nevertheless, by employing buried ridge fabrication in addition to the high-quality optimization of the growth process of Qdash, the characteristic temperature was able to be pushed to as high as T_0 ~135 K on a p-doped 6-stack Qdash-in-barrier laser with twice as high modal gain (11 cm^{-1} per layer) with respect to the undoped laser at the expense of a high threshold current density ~10 kA/cm^2 and internal loss (~60 cm^{-1}) [44]. Furthermore, a drastic improvement in the device dynamic characteristics was witnessed as the relaxation frequency was a high 13.5 GHz which was acquired through RIN measurements (−155 to −160 dB/Hz from 0.5 to 20 GHz) and is among the best reported values in an InAs/InP Qdash material system. Dagens et al. [45] were able to further optimize the design of the Qdash active region by reducing the p- and n-side SCH layers to 20, and 70 nm, respectively in a 6-stack InAs/InGaAsP Qdash laser. This was carried out for the purpose of reducing the carrier transit time and to limit the recovery

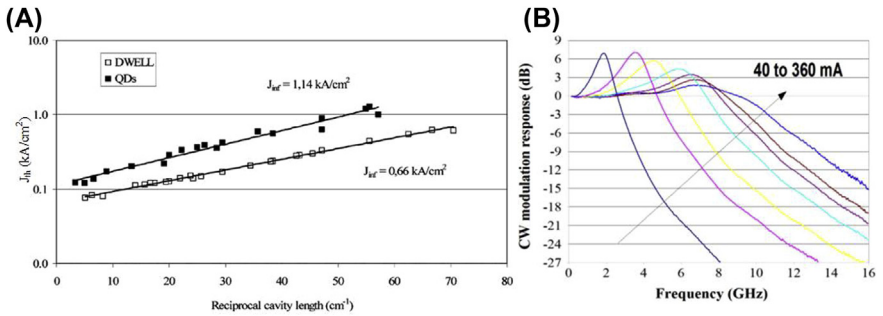

FIG. 5.6

(A) Liner fits in terms of J_{th} as a function of temperature of 2 × 700 μm^2 fixed ridge-waveguide InAs/InGaAsP/InP Qdash laser [43]. (B) Small signal modulation response on a 600 μm as-cleaved, reduced SCH layer thickness buried ridge stripe DaWELL laser at 25 °C. T [45].

From Khan MZM, Ng TK, Ooi BS. Self-assembled InAs/InP quantum dots and quantum dashes: material structures and devices. Progress in Quantum Electronics 2014;38(6):237–313.

of the optical mode and the absorbing p-doped waveguiding layers. The 600 μm long buried ridge-waveguide laser displayed a relatively flat RIN −155 dB/Hz (0.1−16 GHz) whereas the relaxation frequency was estimated as ∼8.5 GHz. More significantly, the obtained small signal modulation bandwidth of 10.5 GHz under CW operation and room temperature is the largest value ever reported on any Qdash material system), as depicted in Fig. 5.6B. Joshi et al. [46] investigated the linewidth enhancement factor associated with p-doping on a 1.25-mm long 6-stack Qdash laser with dashes in InGaAsP Quantum wells and InGaAsP barriers that are p-doped utilizing delta type doping. The distributed feedback laser (DFB) laser demonstrated a significant reduction in the linewidth parameter both below and above threshold (∼2) suggesting that the carrier population in the wetting and barrier layers is reduced leading to a small number of non-resonant carriers.

In a different study, tunneling injection was investigated by Lelarge et al. [47,48] on the InAs/InGaAsP Qdash laser material system. On a buried ridge-waveguide $1.5 \times 600\ \mu m^2$ device, a low 155 A/cm^2 per layer transparency current density and 334 A/cm^2 per layer threshold current density were obtained under CW operation. The slope efficiency and characteristic temperature were estimated as 0.34 W/A and 50 K, respectively, while RIN measurements yielded a value of −155 dB/Hz from 0.1 to 16 GHz. The small signal modulation bandwidth and resonance frequency were measured as ∼8.5 and 4.5 GHz, respectively, with the latter exhibited parasitic-like roll off that was likely related to the carrier transport limitations [48]. The observed minimal impact of tunneling injection scheme on the laser dynamics was likely correlated to the significant carrier escape from the injector-Qdash ensembles. As such, this can be improved with higher energy barriers and carrier confinement or by adopting a moderate p-doping scheme in tandem with tunneling injection as has been adopted by Mi et al. [21] as discussed earlier.

When it comes to the static performance characteristics, Zhou et al. [49,50] reported the smallest value of threshold current density (72 A/cm^2 per layer) and transparency current density (45 A/cm^2 per layer) on a InAs/InGaAsP Qdash material system. The 5-stack Qdash-in-barrier SCH laser structure was grown through the optimized double-cap technique, and employing a 2.2 nm cap with a 30-s growth interruption. The obtained internal quantum efficiency of the ∼1.55−1.58 μm emitting laser was 58% whereas the internal loss was estimated as 7 cm^{-1}. Later on, the lowest internal loss value (2.7 cm^{-1}) on any Qdash material system was reported by Faugeron et al. [51] with a high internal quantum efficiency of 81% on a 6-stack Qdash-in-barrier laser of asymmetric-cladding that was lasing around 1.59 μm. The slope efficiency was estimated as 0.32 W/A whilst the threshold current density was obtained as ∼4 kA/cm^2. Very recently, Pes et al. [34] reported a continuous-wave 1.6 μm-emitting optically-pumped InAs Qdash based vertical-external-cavity surface-emitting laser. In multi-transverse mode operation, the maximum output power was measured as 163 mW at 20 °C from 12 mm-long cavity whereas when the laser was made single-frequency, the maximum measured output power was 7.9 mW at 19.5 °C in a 49 mm-long cavity. The laser device showed a wavelength tunability between 1609 and 1622 nm in the latter condition while the linewidth

was estimated as 22 kHz. Furthermore, Class-A operation was demonstrated with a RIN level of 135 dB/Hz at 100 kHz and a cut-off frequency of 800 kHz.

3.3 InAs/InP Qdash ultra-broadband lasers

Our group was first to demonstrate and exploit the highly inhomogeneous nature of a multi-stack InAs/InGaAlAs Qdash active region [52] as a broadband emitting device. As depicted in Fig. 5.6A, a lasing bandwidth of ~22 nm centered at ~1.64 μm was reported on a 4-stack 50 × 600 μm^2 laser that exhibited a per-layer pulsed threshold current density of 650 A/cm^2 and a slope efficiency of 0.165 W/A with an output power > 400 mW. The emission coverage was able to be pushed later on to 85 nm with a ~41-nm bandwidth by Tan et al. [53] via a 50 × 500 μm^2 as-cleaved intermixed laser that is also shown in Fig. 5.7A. Moreover, a lower threshold current density (525 A/cm^2 per layer) was achieved with a slope efficiency of 0.423 W/A, and a characteristics temperature T_0 ~57. Subsequently, our group successfully reported [6] a record ~50 nm lasing bandwidth and lasing emission coverage of ~65 nm via a chirped barrier 4-stack Qdash active region-based 2 × 830 μm^2 ridge-waveguide laser, as shown in Fig. 5.7B. The laser displayed a per-layer threshold current density of 900 A/cm^2 and a slope efficiency 0.36 W/A. Furthermore, we investigated the device physics of the chirped structure and postulated that simultaneous emission for dispersive Qdashes [33] and the non-uniform distribution of carriers in the Qdash active region [32] play a significant role in the observed broad emission. Very recently, we further investigated the detailed thermal characteristics of the InAs/InP Qdash broadband laser with different ridge widths in terms of junction and characteristics temperatures [54]. The results dictated an inverse relation between the ridge-width and the junction temperature.

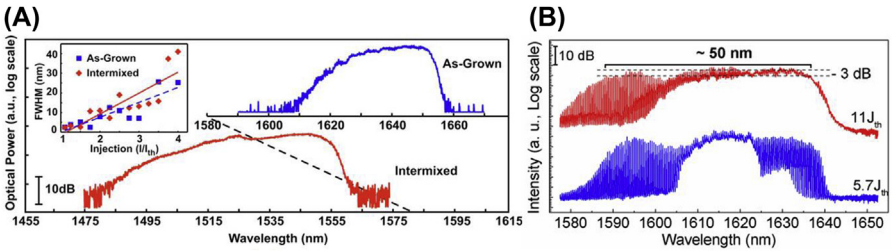

FIG. 5.7

(A) The wavelength tuned broadband fixed barrier 4 stack InAs/InGaAlAs DaWELL laser from 1.64 μm (as-grown) to 1.54 μm (IFVD intermixed) center wavelength. The lasing coverage increases from 76 to 85 nm after the intermixing process. The inset shows the −3 dB bandwidth of the broadband Qdash laser in accordance to injection [53]. (B) Room temperature lasing spectra of 2 × 830 μm^2 chirped barrier thickness 4 stack InAs/InGaAlAs DaWELL laser at different pulsed injection current density [6].

From Khan MZM, Ng TK, Ooi BS. Self-assembled InAs/InP quantum dots and quantum dashes: material structures and devices. Progress in Quantum Electronics 2014;38(6):237–313.

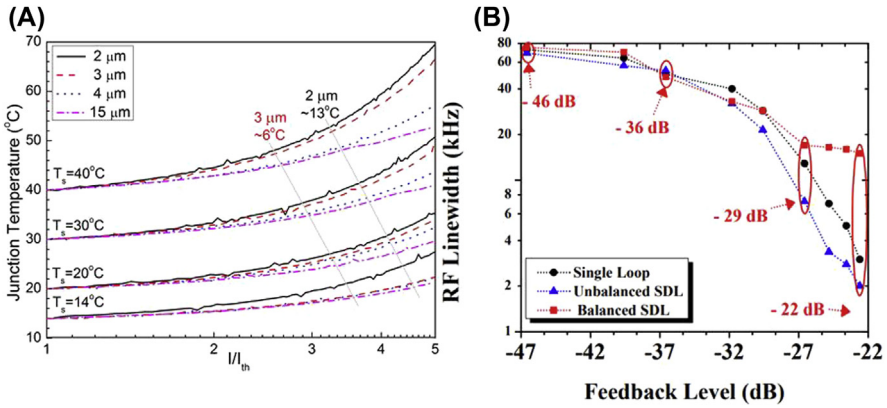

FIG. 5.8

(A) Estimated rise in the junction temperature of all the InAs/InP Qdash laser devices at four different heat sink temperatures, as a function of injection current I/Ith. (B) RF linewidth under resonant condition in the case of single loop, unbalanced and balanced symmetrical dual-loop feedback configurations as a function of external feedback ratio at a bias of 300 mA showing −22 dB to be the optimum value, in the case of single, balanced and unbalanced symmetrical dual-loop feedback configurations.

From Khan MZM, Ng TK, Ooi BS. Self-assembled InAs/InP quantum dots and quantum dashes: material structures and devices. Progress in Quantum Electronics 2014;38(6):237–313. Also reprinted with permission from Asghar H, et al. Stabilization of self-mode-locked quantum dash lasers by symmetric dual-loop optical feedback. Optical Express 2018;26(4):4581–92.

The narrowest 2 μm ridge width which demonstrated the largest lasing bandwidth of ∼ 50 nm, exhibited highest thermal resistance of ∼45 °C/W and hence the largest junction temperature buildup, as illustrated in Fig. 5.8A. This further affirmed thermionic carrier escape and phonon-assisted tunneling to be the dominant carrier transport mechanisms resulting in the non-uniform distribution of carriers, and thus broadband lasing from this device.

3.4 InAs/InP Qdash single mode lasers

On the other hand, few studies have been concocted on single mode Qdash lasers. For the InAs/InGaAlAs material system, Kaiser et al. [55] reported a small signal modulation bandwidth of 7.6 GHz from a 3×1000 μm^2 laterally coupled DFB gratings based on 4 stack InAs/InGaAlAs Qdash laser. The 1.51 μm emitting laser exhibited a slope efficiency and an output power of 0.13 W/A and >30 mW, respectively, whereas the SMSR was estimated as > 40 dB. Later, Zeller et al. [56] and Hein et al. [57] were able to improve the relatively inferior performance of the long wavelength InAs Qdash in InGaAs Qwell DFB lasers as they reported single mode emitting lasers at 2.01 and 1.89 μm, respectively, under CW operation and at room temperature. The former report utilized a 2×900 μm^2 laser with a

threshold current of 40 mA and a high SMSR of >35 dB. The latter one, on the other hand, displayed a slope efficiency 0.22 W/A with an output power >25 mW.

In terms of the InAs/InGaAsP material system, Dagens et al. [58] reported a 4.8 mA threshold current, 45.5 dB SMSR, and a 0.3 W/A slope efficiency from a $0.8 \times 205\ \mu m^2$ a 6-stack DaWELL buried ridge-waveguide DFB laser emitting at 1.51 μm grown via MBE−MOCVD. The small signal modulation bandwidth was obtained as ∼6.7 GHz with a high modulation efficiency of 1.9 GHz/$mA^{0.5}$ and a K-factor 0.43 ns [28]. Subsequently, the direct small signal modulation bandwidth was successfully pushed to ∼10 GHz with a low K-factor of 0.3 ns and a reduced above-threshold LEF of <2 by Lelarge et al. [59]. This was achieved by reducing the SCH layer thickness in a 0.5 mm and 1.0 mm long buried ridge-waveguide DFB lasers emitting at 1.54 μm with a SMSR of ∼40 dB.

3.5 InAs/InP Qdash injection locked laser

Optical injection under stable locking conditions has the potential to enhance the dynamic characteristics of InAs/InP Qdash lasers as has been demonstrated by Li et al. [60] as he reported a three times increase in the small signal modulation bandwidth of $4 \times 500\ \mu m^2$ injection-locked laser. The 3 dB bandwidth at a −8.6 dBm injected power was 8.7 GHz compared to the 3.4 GHz value of the free-running case. Naderi et al. [61] were able to push that value further to 11.7 GHz with a SMSR value of 30 dB corresponding to three times increase over the free-running case. Later, a remarkable 16.5 GHz small signal modulation −3 dB bandwidth was reported by Lester et al. [62]. This four-fold increase in the bandwidth was achieved through a slightly blue shifted (1.535 μm) injection locked Qdash laser under strong optical injection of 9.3 dB. Moreover, a striking near zero above-threshold LEF and a differential gain of $5.9 \times 10^{-14}\ cm^{-2}$ were acquired.

A rigorous dynamic investigation of an injection-locked Qdash laser was subsequently concocted by Pochet et al. [63,64] at zero detuning where it was shown that the a high gain compression coefficient and a large damping rate in addition to a sufficiently small LEF value are operating conditions for stable locking at near-threshold biasing currents. Whilst optical injection can indeed enhance the performance characteristics of Qdash lasers, it can conversely impact the stability of the laser resulting in collapsing the coherence time and broadening the emission spectrum in addition to degrading the LEF and bit error rate (BER). As such, Azouigui et al. [65] investigated the tolerance of Qdash lasers to the optical feedback as it was demonstrated that increasing the current injection of a 205-μm long InAs/InGaAsP Qdash DFB laser from 10 to 100 mA yielded in a coherence collapse from ∼ −41 to −27 dB. Later on, high differential gain devices were shown to have a better performance from this point of view with an onset of coherence collapse as good as >−18 dB [66]. Furthermore, temperature insensitive differential gain laser and/or longer cavity devices were shown to be able to achieve higher optical feedbacks [67]. Contrary to that and opposite to the case with Qwell lasers, Grillot et al. [68] demonstrated that increasing the current injection of a 500-μm long ridge-

waveguide Qdash laser decreased the critical feedback level which was ascribed to the increased non-linear increase of the GS above-threshold LEF from ~1 to ~14 associated with the increased current injection. This since has been adopted as a key parameter in design of Qdash lasers that are feedback-resistant [69]. Sadeev et al. [70] utilized dual-mode optical injection on a single-mode buried InP/InAs Qdash laser with a 1-μm ridge width and emitting at 1.55-μm. A maximum normalized conversion efficiency value of −17 dB was reported with an OSNR of 37 dB at a 27 GHz detuning with a wide detuning range from −1.2 to 2.7 THz.

3.6 InAs/InP Qdash mode-locked lasers

With the aid of mode-locking techniques, the broadly emitting InAs/InP Qdash lasers are capable of sub-picosecond pulse generation which has made them a hot focus of research for the past few years as they have demonstrated remarkable improved performance parameters including, repetition frequency, pulse width, and ultra-small RF linewidth, in the range between <1 kHz and 600 kHz [28,61]. Gosset et al. [71] were first to demonstrate passive mode-locking by utilizing a two-section InAs/InGaAsP Qdash laser where one section acts as a gain section while the other as an absorber. The 6-stack Qdash laser exhibited a RF linewidth of 47 kHz with a gain and absorber sections that are 940 and 180 μm in length, respectively. The resulting pulsation frequency was 43.6 GHz under a CW biasing current of 169 mA. Subsequently, the timing jitter and phase noise were investigated by Dontabactouny et al. [72] on a 1.59 μm emitting 5 stacks InAs/InGaAsP Qdash laser whose gain and absorber sections were 3.95 and 0.13 mm, respectively. With a fixed biasing current and reverse biasing voltage, highly chirped pulses in the range between 8 and 14 ps were generated with a pulsation frequency of 10 GHz by tuning the passband window of a 1 nm bandwidth filter that was centered at 1.6 μm. With the aid of a 545-m long single mode fiber for the purpose of dispersion compensation, the pulses were able to be pushed down to a lowest value of 975 fs after deconvolution. Furthermore, a low timing jitter value of 800 fs was obtained while the phase noise measurements displayed − 80 dBc/Hz at 100 kHz which was then reduced down to −140 dBc/Hz.

Rosales et al. concocted a series of systematic investigations [73–75] on three InAs/InGaAsP Qdash lasers with cavity lengths of 1200, 890, and 450 μm and a 10% absorber section. The obtained respective repetition rates were 20, 48 and 95 GHz with the latter value being the highest reported on any InAs/InP Qdash monolithic two-section device. Mode-locking was achieved at a fairly large reverse bias with deconvolved pulse durations of ~1.4, ~2.5 and ~1.6 ps for the long, medium, and short devices respectively. Recently, Asghar et al. [76] analyzed in detail the effects of optical feedback single- and dual-loops on the pulse trains generated by a two-sectioned Qdash laser emitting at 1.55 μm with a repetition range of ~ 20 GHz. The investigation aimed to identify the optimal feedback level that achieves minimum RF linewidth and hence lowest timing jitter. As Fig. 5.8B shows, a ~−22 dB feedback level was shown to achieve a high suppression of the RF

linewidth from 98 kHz (in the case of free-running) to 5 and 1.5 kHz for the single- and dual-loop configurations, respectively. Moreover, the corresponding timing jitter was measured as ∼800 and ∼500 fs for the single- and dual-loop configurations, respectively, compared to the ∼4.8 ps associated with the free-running case. Very recently, it was demonstrated that [77] employing an unbalanced symmetric dual-loop configuration in tandem with a full tuning of delay phase of the second feedback cavity resulted in narrower RF linewidths (1.5 kHz) and reduced timing jitter (450 fs) across the widest delay range at the same optical feedback level of a ∼−22 dB when compared to single (3 kHz RF linewidth and 600 fs timing jitter) and balanced symmetric dual-loop feedback systems.

Compared to two-section mode locking, passive singe-section mode locking (self-pulsation) is more favorable from different points of view, such as achievable power and pulse width, and thus have been adopted by researchers for the past decade showing a superior performance. As such, Gosset et al. [71] were first to report a mono-section mode locking in a Qdash material system. A 134 GHz pulse generation was reported on a 6-stack 340 μm long InAs/InGaAsP DaWELL laser operating at 1.56 μm under CW bias. A sub-picosecond pulse width of 800 fs without deconvolution or pulse compression was measured with a 50 kHz RF spectral linewidth. Moreover, the pulse repetition rate was reported to be 42.2 GHz with 2 ps auto-correlated pulses. Shen et al. [78] demonstrated the viability in employing optical filters in order to limit the beating linewidth to 2 kHz on a 17 GHz, 2.5 mm long Qdash mode-locked laser (QD-MLL). Later on, reducing the optical confinement factor was show to have a similar effect on the beating linewidth [79]. It was postulated that this was owning to the reduced optical mode interactions with the amplified spontaneous emission, and large population inversion, leading to a reduced phase noise [73,80].

Alternatively, the mode-beating linewidth (phase noise) was reduced from 30 kHz (−75 dBc/Hz) to a mere 200 Hz (−105 dBc/Hz) by Akrout et al. [81] via employing an external cavity length based high quality factor in an auto-optical feedback loop for initial phase noise reduction. This was carried out on a self-pulsating 30.3 GHz InAs/InGaAsP/InP QD-MLL. In terms of the timing jitter, Latkowski et al. [82] utilized a 450-m long single mode dispersion-compensated fiber and demonstrated 720-fs wide pulses via a 39.8 GHz QD-MLL. Moreover, independently of the biasing current, a beating linewidth of 10−25 kHz was obtained with a timing jitter that varied from 350 to 150 fs while the peak power varied from 40 to 140 mW [83,84], as shown in Fig. 5.9A. It was found that increasing the bias current or the filter bandwidth resulted in a reduction in the pulse width which was ascribed to the superior phase locking at higher injection and larger number of locked longitudinal modes [85,86].

On another front, a record repetition rate of 346 GHz was reported by Merghem et al. [87] as depicted in see Fig. 5.9B by employing a 120-μm long Qdash laser emitting ∼560 fs deconvolved pulses of a peak power of 20 mW and an extinction ratio of 9 dB. Later on, a detailed investigation [88] on the repetition frequency stability was carried out on a 10 GHz Qdash passively mode-locked laser. Furthermore,

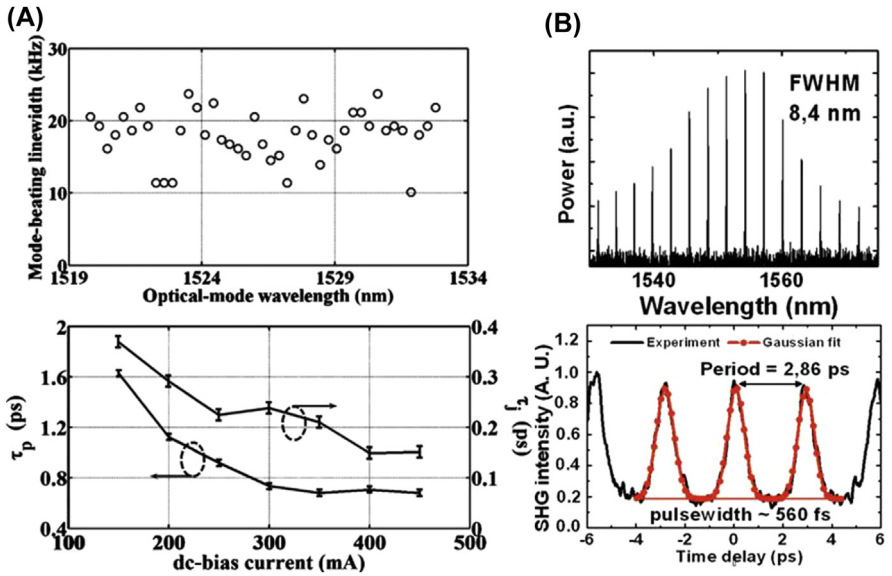

FIG. 5.9

(A) Typical mode-beating associated with each pair of optical modes as a function of the filter central wavelength (top) of the 1000 μm long 40 GHz InAs/InGaAsP Qdash mode-locked laser at 350 mA. The corresponding device pulse width and timing jitter associated with the optically generated pulses as a function of CW current (bottom) [84]. (B) Optical spectrum (top) and autocorrelation trace (bottom) of 120 μm long, 345 GHz, InAs/InGaAsP Qdash mode-locked laser at 217 mA [87].

From Khan MZM, Ng TK, Ooi BS. Self-assembled InAs/InP quantum dots and quantum dashes: material structures and devices. Progress in Quantum Electronics 2014;38(6):237–313.

an electrical and an optical feedback loops were developed and demonstrated to improve the initial long-term stability of the free-running case $\sim 10^{-7}$ to a long-term stability of 3×10^{-9} in the case of the electrical feed-back system and to 1.5×10^{-9} in the case of the optical feed-back system.

By employing the second-harmonic generation frequency resolved optical gating (SHG-FROG) technique, Calò et al. [89] investigated a high gain $\sim 50\ \text{cm}^{-1}$, 890-μm long device, 9-stack InAs/InGaAsP dash-in-barrier laser. The 1.56 μm emitting device showed a ~48 GHz repetition frequency under CW operation. Highly chirped 423 fs pulses were achieved through a single mode fiber with a peak power of ~100 mW peak power at 300 mA biasing current. This was however was further reduced later [90] to 374 fs at 400 mA which is the best reported value on any InAs/InP Qdash material system. Later, a record peak power of 18 W was reported by Faugeron et al. [51] by developing an asymmetrical cladding 10-mm long, 4.4 GHz, single-section Qdash laser with a narrow RF linewidth of 300 Hz. The Qdash laser emitted 750 fs deconvolved pulses post-compression and 9.3 ps/nm

compensation via a 570-m long single mode fiber. Furthermore, an improved phase noise <-100 dB/Hz at an offset frequency of 1 kHz and RF harmonics up to 120 GHz were also reported on a 4.3-mm long Qdash laser [29].

In another study, Sooudi et al. [91] utilized double locking with simultaneous optical injection and optical feedback on QD-MLL and reported a reduction of two times in the bandwidth product and two orders of magnitude reduction in the RF linewidth. This work was followed by an implementation of dual-loop feedback in tandem with optical injection and optical fiber delay by Wei et al. [92] on a 1.55 μm, 20 GHz InAs/InP DaWELL. As such, the RF linewidth and timing jitter were significantly reduced from 97.9 kHz to 4.27 ps, respectively in the case of free-running, to 972 Hz and 430 fs. Moreover, a reduction in the phase noise from -74 dBc/Hz to -87 dBc/Hz at100 kHz frequency offset was also reported.

4. InAs/InP Qdash lasers in optical communications

Over the past decade, network traffic and increases in consumer demands are producing significant challenges to continue optical communications on cost-effective scale. In today's digital information society, large number of applications demands high bit rate to accommodate individual users. Several hundred Terabit/s per chip will be required for next generation system architectures over the next few years. Meeting those demands will require new forms of optical solutions. One of the promising solutions are addressed by the employment of Qdash based mode-locked or injection-locked lasers as multiwavelength or transmitter sources for WDM system, owing to their notable broadband lasing emission properties with reduced RIN. This feature of Qdash lasers appears to be highly attractive for next-generation passive optical networks (NG-PONs) as well. In this section, we discuss various demonstration of employment of Qdash lasers in as a source in optical communications.

4.1 InAs/InP Qdash mode-locked lasers

Akrout et al. was the first to propose and demonstrate 10 Gb/s on-off keying (OOK) transmission of eight WDM channels via a single QD-MLL over 50-km single-mode fiber (SMF) [93]. As compared to the single-mode distributed feedback laser, a WDM comb generation emitting at 1.55 μm was utilized with 100-GHz channel spacing. Subsequently, QD-MLL as seeding light source was reported by Nguyen et al. [94] for colorless WDM passive optical networks. A bidirectional transmission of 2.5 Gb/s was demonstrated for 16 WDM channels over 25 km SMF in the C-band. As a coherent multiwavelength seeding source, a QD-MLL is optically injected into wavelength-locked typical Fabry-Perot laser diode (FP-LD) with mode spacing of 42.7-GHz.

Taking advantages of mode-locked laser diodes, M. Costa e Silva et al. [95] demonstrated first 4×170 Gb/s capacity dense WDM transmission using single

QD-MLL source. The four channels were transmitted over 100 SMF length. Later, comb generation with nine *C*-band WDM channels were investigated by M'Sallem et al. [96]. An external modulation of 56 Gb/s differential quaternary phase-shift keying (DQPSK) transmission was reported based on 100-GHz WDM grid using a single QD-MLL for broadcast applications. Later, Gay et al. demonstrated 112 Gb/s WDM transmission of four dense WDM (DWDM) channels using a single QD-MLL followed by a SOA in order to reduce mode partition noise [97]. Each channel is directly modulated at 28 Gb/s in OOK format after 100 km fiber. Alternatively, feed forward heterodyne [98] and self-homodyne [99] detection schemes were employed by J. Pfeifle et al. to reduce the phase noise and optical linewidth of QD-MLL. In Ref. [98], coherent Tbit/s transmission was demonstrated on simultaneous 30 comb lines at 18 Gbaud QPSK signal and over 75 km fiber, with an aggregate capacity of $\sim$ 1 Tbit/s. This was further enhanced to an aggregate data rate of 1.562 Tbit/s with 25 comb lines of QD-MLL via 16 QAM transmission, and at a symbol rate of 18 Gbaud, utilizing self-homodyne system [99].

Recently, by employing optimized QD-MLL with potential applications in data center optical interconnects, Vujicic et al. [100] achieved an aggregate data capacities of 1.128 Tb/s and 2.256 Tb/s for 44.7 GHz and 22.7 GHz free spectral ranges (FSRs) devices, respectively. WDM transmission of 28.2 Gb/s was demonstrated over 3 km SMF through 40 (44.7 GHz FSR) and 80 (22.7 GHz FSR) channels using intensity modulation/direct detection (IM/DD) scheme. Moreover, they extended their work with long distance transmission of 50 km SMF employing 16 (shown in Fig. 5.9), 40 and 80 channels from a single QD-MLL, achieving an aggregate capacity up to 4.5 Tb/s for interconnect applications [101]. Fig. 5.10A showed the measured lasing spectrum of 82.8 GHz QD-MLL with $\sim$ 4 dB flatness. Bit error rate was measured to determine the channel performance at received optical power of $\sim$0 dBm. The results obtained after transmission of 3 km and 50 km are shown in Fig. 5.10B below the 7% (BER: 4×10^{-3}) and 20% (BER: 1.6×10^{-2}) forward-error correction (FEC) thresholds, respectively. Fig. 5.10C shows the measured RIN of all 16 modes, with an average measured value from -131 to -134 dB/Hz. The constellation diagram for 8 middle channels after 3 km transmission is shown in Fig. 5.10D.

In terms of the highest data rate in *C*-band and high order modulation format, Kemal et al. [102] reported net data rate of 12 Tb/s by employing resonant feedback in QD-MLL. The transmission experiment utilized 32 QAM modulation scheme with a symbol rate of 20 Gbaud over 75 km SMF. Fig. 5.11A shows the combined spectrum of odd and even channels before modulation (P1) and after modulation (P2), as total of 60 channels were used out of the complete QD-MLL spectrum. The measured BER for seven random channels for back-to-back (BtB) and 75 km fiber transmission for all channels is shown in Fig. 5.11B which are below the 7% of FEC BER threshold. To compensate high demand of bandwidth-hungry multiple services, Rosales et al. [103] also demonstrated the potential of QD-MLL for radio-over-fiber broadband wireless communication. A direct modulation of 3 Gb/s QAM transmission was demonstrated for short indoor communication.

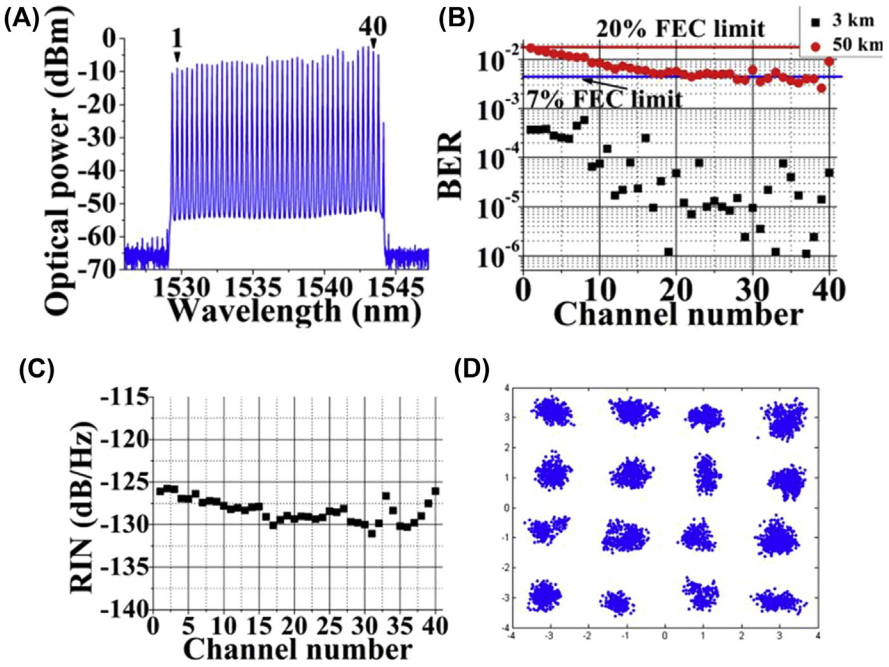

FIG. 5.10

(A) Optical spectrum of Qdash MLL (FSR: 44.7 GHz) (B) measured bit error rate for each channel over 3 km and 50 km fiber transmission (C) Relative intensity noise (RIN) of all modes (D) the constellation diagram over 3 km of SMF of middle channel.

Reprinted with permission from Vujicic V, Calò C, Watts R, Lelarge F, Browning C, Merghem K, Martinez A, Ramdane A, Barry LP. Quantum dash mode-locked lasers for data centre applications. IEEE Journal of Selected Topics in Quantum Electronics 2015;21(6):53–60.

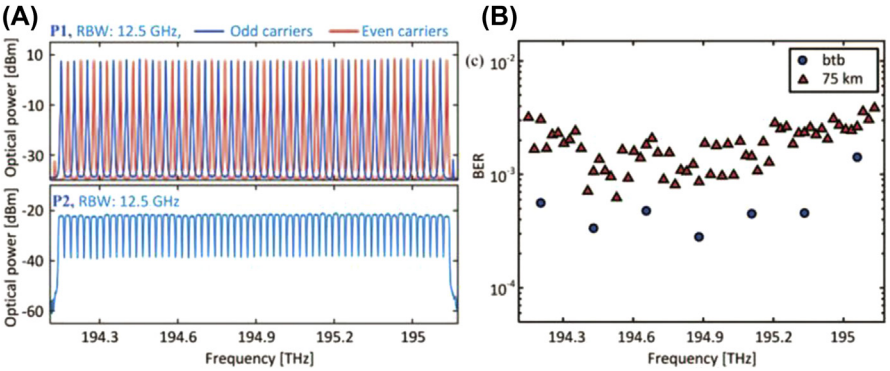

FIG. 5.11

(A) Optical spectra of even and odd channels before modulation (P1), 60 modulated channels (P2) of InAs/InP Qdash MLL (B) Measured bit error rate for BtB and 75 km fiber transmission.

Reprinted with permission from Kemal JN, Marin-Palomo P, Merghem K, Aubin G, Calo C, Brenot R, Lelarge F, et al. 32QAM WDM transmission using a quantum-dash passively mode-locked laser with resonant feedback. In: 2017 optical fiber communications conference and exhibition (OFC); 2017. p. 1–3.

4.2 InAs/InP Qdash injection-locked lasers

Employment of injection-locked InAs/InP Qdash lasers as a transmitter source for next-generation WDM passive optical networks were explored by our group where Khan et al. successfully reported a record 100 Gb/s transmission capacity in the far *L*-band, on a single injection-locked channel [104]. The measured single externally-locked Fabry-Perot mode at ~1621 nm along with free running spectrum of Qdash laser diode, centered at ~1625 nm is shown in Fig. 5.12A. Moreover, a mode wavelength tunability of ~23 nm, capable of encompassing ~50 sub-carriers, was also reported, which would enable an aggregate transmission capacity of ~5 Tb/s using single QD-LD if injection-locked simultaneously. The measured BER at 32, 64 and 100 Gb/s are presented in Fig. 5.12B, which demonstrated the successful transmission below FEC threshold (BER: 3.8×10^{-3}) in BtB and over 10-km SMF while utilizing dual polarization QPSK (DP-QPSK) modulation technique. Alternatively, an injection-locked QD-LD source has also been experimentally demonstrated for future high speed free space optical communication (FSO) by Khan et al. [105]. A single channel 100 Gb/s FSO transmission over 4 m and 2 m FSO channel was reported in L-band wavelength region. These results demonstrated the potential of far L-band QD-LD as a transmitter source for both fiber and wireless communication.

In addition, our group [106] exploited the self-injection locking scheme to demonstrate a multi-wavelength QD-LD with mode selectivity from 1 to 16

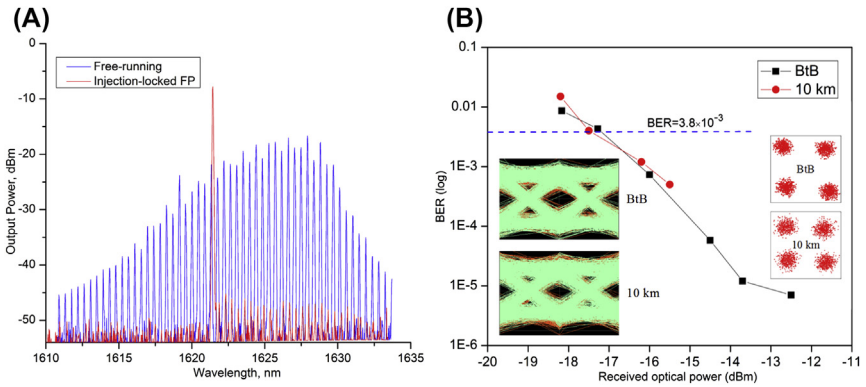

FIG. 5.12

(A) Optical spectra of injection-locked InAs/InP QD-LD (red) and free-running characteristics (blue). (B) Measured BER for 100 Gb/s after BtB and 10 km transmission. Insets show the corresponding QPSK constellations and the eye diagrams.

Reprinted with permission from Khan MTA, et al. 100 Gb/s single channel transmission using injection-locked 1621 nm quantum-dash laser. IEEE Photonics Technology Letters 2017;29(6):543–6.

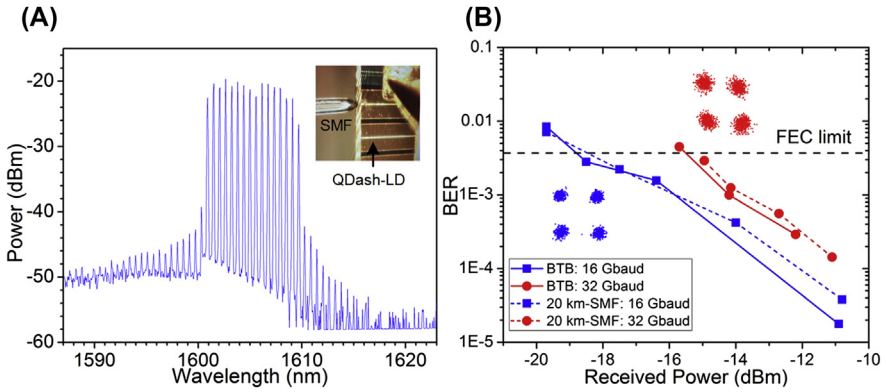

FIG. 5.13

(A) Optical spectrum of the multiwavelength self-injection locked QD-LD, exhibiting simultaneous 16 locked modes. (B) Measured BER for single self-injection locked mode at 1609.6 nm for 64 Gb/s (blue) and 128 Gb/s (red) over BtB and 20 km SMF transmission. The insets show the corresponding constellations of both data rates at −11 dBm received power.

Reprinted with permission from Shemis MA, Ragheb AM, Khan MTA, Fathallah HA, Alshebeili S, Qureshi KK, Khan MZM. L-band quantum-dash self-injection locked multiwavelength laser source for future WDM access networks. IEEE Photonics Journal 2017;9(5):1–7.

channels or locked FP modes in mid *L*-band wavelengths, as shown in Fig. 5.13A. Using a single self-seeded mode a successful transmission of up to 128 Gb/s DP-QPSK over 20 km SMF was reported with measured BER below the FEC limit, as depicted in Fig. 5.13B, with clear constellation diagrams for both transmission rates. Moreover, Shemis et al. also investigated the deployment of this multiwavelength self-seeded QD-LD for future access optical access networks by proposing a plausible next generation PON [106], and over an indoor 5 m FSO channel [107] in mid L-band, with a potential aggregate capacity of 1.28 Tb/s.

Acknowledgments

Authors EAA, MTAK and MZMK gratefully acknowledges the support from King Fahd University of Petroleum and Minerals (KFUPM) grants, SR141002, SR161029 and KAUST004, while TKN, MZMK, and BSO acknowledge the financial support from the King Abdulaziz City for Science and Technology (KACST), Grant No. KACST TIC R2-FP-008. King Abdullah University of Science and Technology (KAUST) funding, BAS/1/1614-01-01, C/M-20000-12-001-77. KCR/1/2081-01-01, and GEN/1/6607-01-01. All the authors acknowledge the funding support from KAUST-KFUPM Special Initiative (KKI) Program, EE2381 and REP/1/2878-01-01.

References

[1] Bimberg D, Grundmann M, Ledentsov NN. Quantum dot heterostructures. John Wiley & Sons; 1999.

[2] Zhukov A, Maksimov M, Kovsh A. Device characteristics of long-wavelength lasers based on self-organized quantum dots. Semiconductors 2012;46:1225−50.

[3] Wang R, Stintz A, Varangis P, Newell T, Li H, Malloy K, et al. Room-temperature operation of InAs quantum-dash lasers on InP [001]. IEEE Photonics Technology Letters 2001;13:767−9.

[4] Reithmaier JP, Eisenstein G, Forchel A. InAs/InP quantum-dash lasers and amplifiers. Proceedings of the IEEE 2007;95(9):1779−90.

[5] Khan MZM, Ng TK, Ooi BS. Self-assembled InAs/InP quantum dots and quantum dashes: material structures and devices. Progress in Quantum Electronics 2014;38: 237−313.

[6] Khan MZM, Ng TK, Lee C-S, Bhattacharya P, Ooi BS. Chirped InAs/InP quantum-dash laser with enhanced broad spectrum of stimulated emission. Applied Physics Letters 2013;102:091102.

[7] Hsieh Y-S, Ho Y-C, Lee S-Y, Chuang C-C, Tsai J-C, Lin K-F, et al. Dental optical coherence tomography. Sensors 2013;13:8928−49.

[8] Ishida S, Nishizawa N. Quantitative comparison of contrast and imaging depth of ultrahigh-resolution optical coherence tomography images in 800−1700 nm wavelength region. Biomedical Optics Express 2012;3:282−94.

[9] Kodach V, Kalkman J, Faber D, Van Leeuwen T. Quantitative comparison of the OCT imaging depth at 1300 nm and 1600 nm. Biomedical Optics Express 2010;1:176−85.

[10] Sharma U, Chang EW, Yun SH. Long-wavelength optical coherence tomography at 1.7 μm for enhanced imaging depth. Optics Express 2008;16:19712−23.

[11] Scholle K, Lamrini S, Koopmann P, Fuhrberg P. 2 μm laser sources and their possible applications. In: Frontiers in guided wave optics and optoelectronics. INTECH; 2010.

[12] Guo S, Ohno H, Shen A, Matsukura F, Ohno Y. InAs self-organized quantum dashes grown on GaAs (211) B. Applied Physics Letters 1997;70:2738−40.

[13] Utzmeier T, Postigo PA, Tamayo J, Garcia R, Briones F. Transition from self-organized InSb quantum-dots to quantum dashes. Applied Physics Letters 1996;69:2674−6.

[14] Li H, Wu J, Wang Z, Daniels-Race T. High-density InAs nanowires realized in situ on (100) InP. Applied Physics Letters 1999;75:1173−5.

[15] Li H, Zhuang Q, Kong X, Wang Z, Daniels-Race T. Self-organization of wire-like InAs nanostructures on InP. Journal of Crystal Growth 1999;205:613−7.

[16] Schwertberger R, Gold D, Reithmaier J, Forchel A. Epitaxial growth of 1.55 μm emitting InAs quantum dashes on InP-based heterostructures by GS-MBE for long-wavelength laser applications. Journal of Crystal Growth 2003;251:248−52.

[17] Rotter T, Stintz A, Malloy K. InP based quantum dash lasers with 2 μm wavelength. IEEE Proceedings - OptoElectronics 2003:318−21.

[18] Sauerwald A, Kummell T, Bacher G, Somers A, Schwertberger R, Reithmaier J, et al. Size control of InAs quantum dashes. Applied Physics Letters 2005;86: 253112−253112-3.

[19] Sauerwald A, Kümmell T, Löffler A, Somers A, Reithmaier J, Forchel A, et al. Scanning transmission electron microscopy of vertically stacked self organized quantum structures. Physica Status Solidi 2006;3:3947−50.

[20] Mi Z, Yang J, Bhattacharya P. Growth and characteristics of P-doped InAs tunnel injection quantum-dash lasers on InP. IEEE Photonics Technology Letters 2006;18: 1377−9.
[21] Podemski P, Sek G, Ryczko K, Misiewicz J, Hein S, Höfling S, et al. Columnar quantum dashes for an active region in polarization independent semiconductor optical amplifiers at 1.55μm. Applied Physics Letters 2008;93.
[22] González L, García JM, García R, Briones F, Martínez-Pastor J, Ballesteros C. Influence of buffer-layer surface morphology on the self-organized growth of InAs on InP(001) nanostructures. Applied Physics Letters 2000;76:1104−6.
[23] Garcıa J, González L, González MU, Silveira JP, González Y, Briones F. InAs/InP (001) quantum wire formation due to anisotropic stress relaxation: in situ stress measurements. Journal of Crystal Growth 2001;227:975−9.
[24] Gendry M, Monat C, Brault J, Regreny P, Hollinger G, Salem B, et al. From large to low height dispersion for self-organized InAs quantum sticks emitting at 1.55 μm on InP (001). Journal of Applied Physics 2004;95:4761−6.
[25] Fuster D, González L, González Y, González MU, Martínez-Pastor J. Size and emission wavelength control of InAs/InP quantum wires. Journal of Applied Physics 2005; 98:033502.
[26] Alén B, Martínez-Pastor J, González L, García JM, Molina SI, Ponce A, et al. Size-filtering effects by stacking InAs/InP (001) self-assembled quantum wires into multilayers. Physical Review B 2002;65:241301.
[27] Lelarge F, Dagens B, Renaudier J, Brenot R, Accard A, van Dijk F, et al. Recent advances on InAs/InP quantum dash based semiconductor lasers and optical amplifiers operating at 1.55 μm. IEEE Journal of Selected Topics in Quantum Electronics 2007;13:111−24.
[28] Faugeron M, Tran M, Lelarge F, Chtioui M, Robert Y, Vinet E, et al. High power mode locked quantum dash 1.5 μm laser with asymmetrical cladding. In: CLEO: science and innovations; 2012. JW2A.85.
[29] Deubert S, Somers A, Kaiser W, Schwertberger R, Reithmaier J, Forchel A. InP-based quantum dash lasers for wide gain bandwidth applications. Journal of Crystal Growth 2005;278:346−50.
[30] Reithmaier J, Somers A, Deubert S, Schwertberger R, Kaiser W, Forchel A, et al. InP based lasers and optical amplifiers with wire-/dot-like active regions. Journal of Physics D: Applied Physics 2005;38:2088.
[31] Tan C, Djie H, Tan C, Hongpinyo V, Ding Y, Ooi B. The effect of multi active junctions on broadband emission from InAs/InGaAlAs quantum-dash structure. In: LEOS annual meeting conference proceedings, 2009. LEOS'09. IEEE; 2009. p. 147−8.
[32] Khan MZM, Ng T, Lee C-S, Anjum D, Cha D, Bhattacharya P, et al. Distinct lasing operation from chirped InAs/InP quantum-dash laser. IEEE Photonics Journal 2013; 5:1501308.
[33] Khan MZM, Ng TK, Lee C-S, Bhattacharya P, Ooi BS. Investigation of chirped InAs/InGaAlAs/InP quantum dash lasers as broadband emitters. IEEE Journal of Quantum Electronics 2014;50:51−61.
[34] Pes S, Paranthoën C, Levallois C, Chevalier N, Hamel C, Audo K, Loas G, Bouhier S, Gomez C, Harmand J, Bouchoule S, Folliot H, Alouini M. Class-A operation of an optically-pumped 1.6 μm-emitting quantum dash-based vertical-external-cavity surface-emitting laser on InP. Optics Express 2017;25:11760−6.

[35] Schwertberger R, Gold D, Reithmaier J, Forchel A. Long-wavelength InP-based quantum-dash lasers. IEEE Photonics Technology Letters 2002;14:735−7.
[36] Resneau P, Calligaro M, Bansropun S, Parillaud O, Krakowski M, Schwertberger R, et al. High-power and low-noise 1.55 μm InP-based quantum dash lasers. In: SPIE photonics Europe; 2004. p. 22−32.
[37] Resneau P, Calligaro M, Krakowski M, Liu H, Hopkinson M, Somers A, et al. High power and very low noise operation at 1.3 and 1.5 μm with quantum dot and quantum dash Fabry-Perot lasers for microwave links. In: Optics/photonics in security and defence; 2006. 63990K−63990K-12.
[38] Hein S, Hofling S, Forchel A. Modulation bandwidth and linewidth enhancement factor of high-speed 1.55-m quantum-dash lasers. IEEE Photonics Technology Letters 2009;21:528−30.
[39] Hein S, Podemski P, Sek G, Misiewicz J, Ridha P, Fiore A, et al. Orientation dependent emission properties of columnar quantum dash laser structures. Applied Physics Letters 2009;94:241113.
[40] Djie HS, Wang Y, Ooi BS, Wang D-N, Hwang J, Dang GT, et al. Defect annealing of InAs-InAlGaAs quantum-dash-in-asymmetric-well laser. IEEE Photonics Technology Letters 2006;18:2329−31.
[41] Rudno-Rudziński W, Syperek M, Andrzejewski J, Maryński A, Misiewicz J, Somers A, Höfling S, Reithmaier JP, Sek G. Carrier delocalization in InAs/InGaAlAs/InP quantum-dash-based tunnel injection system for 1.55 μm emission. AIP Advances 2017;7:015117.
[42] Moreau G, Azouigui S, Cong D-Y, Merghem K, Martinez A, Patriarche G, et al. Effect of layer stacking and p-type doping on the performance of InAs/InP quantum-dash-in-a-well lasers emitting at 1.55 μm. Applied Physics Letters 2006;89:241123−241123-3.
[43] Moreau G, Martinez A, Merghem K, Guilet S, Bouchoule S, Patriarche G, et al. InAs/InP quantum dash based electro optic modulator with over 70 nm bandwidth at 1.55 μM. In: IEEE 19th international conference on indium phosphide & related materials, 2007. IPRM'07; 2007. p. 271−3.
[44] Lelarge FB, Rousseau R, Martin B, Poingt F, LeGouezigou F, Le Gouezigou OPL. Effect of P-doping on temperature and dynamic performances of 1550nm InAs/InP Quantum Dash based lasers. 2009.
[45] Dagens B, Make D, Lelarge F, Rousseau B, Calligaro M, Carbonnelle M, et al. High bandwidth operation of directly modulated laser based on quantum-dash InAs−InP material at 1.55 m. IEEE Photonics Technology Letters 2008;20:903−5.
[46] Joshi S, Chimot N, Ramdane A, Lelarge F. On the nature of the linewidth enhancement factor in p-doped quantum dash based lasers. Applied Physics Letters 2014;105:241117.
[47] Duan GH, Shen A, Akrout A, Dijk FV, Lelarge F, Pommereau F, et al. High performance InP-based quantum dash semiconductor mode-locked lasers for optical communications. Bell Labs Technical Journal 2009;14:63−84.
[48] Lelarge F, Rousseau B, Martin F, Poingt F, Le Gouezigou L, Le Gouezigou O, et al. Optimization of tunneling-injection InAs/InP (100) quantum dashes lasers for high-speed optoelectronic devices. In: IEEE 19th international conference on indium phosphide & related materials, 2007. IPRM'07; 2007. p. 274−7.

[49] Zhou D, Piron R, Dontabactouny M, Dehaese O, Grillot F, Batte T, et al. Low threshold current density of InAs quantum dash laser on InP (100) through optimizing double cap technique. Applied Physics Letters 2009;94:081107.
[50] Zhou D, Piron R, Dontabactouny M, Dehaese O, Grillot F, Batte T, et al. Low-threshold current density InAs quantum dash lasers on InP (100) grown by molecular beam epitaxy. Electronics Letters 2009;45:50−1.
[51] Faugeron M, Lelarge F, Tran M, Robert Y, Vinet E, Enard A, et al. High peak power, narrow RF linewidth asymmetrical cladding quantum-dash mode-locked lasers. IEEE Journal of Selected Topics in Quantum Electronics 2013;19.
[52] Djie HS, Tan CL, Ooi BS, Hwang J, Fang X-M, Wu Y, et al. Ultrabroad stimulated emission from quantum-dash laser. Applied Physics Letters 2007;91: 111116−111116-3.
[53] Tan C, Djie HS, Wang Y, Dimas CE, Hongpinyo V, Ding YH, et al. Wavelength tuning and emission width widening of ultrabroad quantum dash interband laser. Applied Physics Letters 2008;93:111101.
[54] Alkhazraji E, Khan MTA, Khan MZM. Effect of temperature and ridge-width on the lasing characteristics of InAs/InP quantum-dash lasers: a thermal analysis view. Optics & Laser Technology 2018;98:67−74.
[55] Kaiser W, Mathwig K, Deubert S, Reithmaier J, Forchel A, Parillaud O, et al. Static and dynamic properties of laterally coupled DFB lasers based on InAs/InP QDash structures. Electronics Letters 2005;41:808−10.
[56] Zeller W, Legge M, Somers A, Kaiser W, Koeth J, Forchel A. Singlemode emission at 2 μm wavelength with InP based quantum dash DFB lasers. Electronics Letters 2008; 44:354−6.
[57] Hein S, Somers A, Kaiser W, Höfling S, Reithmaier J, Forchel A. Singlemode InAs/InP quantum dash distributed feedback lasers emitting in 1.9 μm range. Electronics Letters 2008;44:527−8.
[58] Dagens B, Make D, Le Gouezigou O, Provost J, Lelarge F, Accard A, et al. First demonstration of 10 Gb/s direct modulation with a buried ridge distributed feedback laser based on quantum dash InAs/InP material at 1.55 μm. In: European conference on optical communications, 2006. ECOC 2006; 2006. p. 1−2.
[59] Lelarge F, Chimot N, Rousseau B, Martin F, Brenot R, Accard A. Chirp optimization of 1550nm InAs/InP Quantum Dash based directly modulated lasers for 10Gb/s SMF transmission up to 65Km. In: International conference on indium phosphide & related materials (IPRM), 2010; 2010. p. 1−3.
[60] Li YN, Kovanis N, V Lester L. Modulation response of an injection-locked 1550 nm quantum dash semiconductor laser. 2007.
[61] Naderi NA, Pochet M, Grillot F, Terry NB, Kovanis V, Lester LF. Modeling the injection-locked behavior of a quantum dash semiconductor laser. IEEE Journal of Selected Topics in Quantum Electronics 2009;15:563−71.
[62] Lester LF, Naderi NA, Grillot F, Raghunathan R, Kovanis V. Strong optical injection and the differential gain in a quantum dash laser. Optics Express 2014;22:7222−8.
[63] Pochet M, Naderi N, Terry N, Kovanis V, Lester L. Dynamic behavior of an injection-locked quantum-dash Fabry-Perot laser at zero-detuning. Optics Express 2009;17: 20623−30.
[64] Pochet MC, Naderi NA, Kovanis V, Lester LF. Modeling the dynamic response of an optically-injected nanostructure diode laser. IEEE Journal of Quantum Electronics 2011;47:827−33.

[65] Azouigui S, Dagens B, Lelarge F, Provost J, Accard A, Grillot F, et al. Tolerance to optical feedback of 10-gb/s quantum-dash-based lasers emitting at 1.51 μm. IEEE Photonics Technology Letters 2007;19:1181−3.
[66] Azouigui S, Dagens B, Lelarge F, Accard A, Make D, Le Gouezigou O, et al. Systematic investigation of InAs/InP quantum-dash based lasers under external optical feedback. Applied Physics Letters 2008;92:201106−201106-3.
[67] Azouigui S, Dagens B, Lelarge F, Provost J, Make D, Le Gouezigou O, et al. Optical feedback tolerance of quantum-dot-and quantum-dash-based semiconductor lasers operating at 1.55 m. IEEE Journal of Selected Topics in Quantum Electronics 2009; 15:764−73.
[68] Grillot F, Naderi NA, Pochet M, Lin C-Y, Lester LF. Variation of the feedback sensitivity in a 1.55 μm InAs/InP quantum-dash Fabry−Perot semiconductor laser. Applied Physics Letters 2008;93:191108−191108-3.
[69] Grillot F, Naderi NA, Pochet M, Lin C-Y, Besnard P, Lester LF. Tuning of the critical feedback level in 1.55-μm quantum dash semiconductor laser diodes. IET Optoelectronics 2009;3:242−7.
[70] Sadeev T, Huang H, Shires K, Arsenijević D, Grillot F, Bimberg D. Non-linear and dynamic properties of MOVPE-grown InAs/InP quantum-dot and quantum-dash Fabry-Perot lasers. In: 2015 IEEE Photonics conference (IPC), Reston, VA; 2015. p. 607−8.
[71] Gosset C, Merghem K, Martinez A, Moreau G, Patriarche G, Aubin G, et al. Subpicosecond pulse generation at 134 GHz using a quantum-dash-based Fabry-Perot laser emitting at 1.56 μm. Applied Physics Letters 2006;88:241105−241105-3.
[72] Dontabactouny M, Rosenberg C, Semenova E, Larsson D, Yvind K, Piron R, et al. 10-GHz 1.59-μm quantum dash passively mode-locked two-section lasers. In: SPIE photonics Europe; 2010. 77201A−77201A-10.
[73] Rosales R, Merghem K, Martinez A, Akrout A, Tourrenc J-P, Accard A, et al. InAs/InP quantum-dot passively mode-locked lasers for 1.55-μm applications. IEEE Journal of Selected Topics in Quantum Electronics 2011;17:1292−301.
[74] Rosales R, Merghem K, Martinez A, Accard A, Lelarge F, Ramdane A. High repetition rate two-section InAs/InP quantum-dash passively mode locked lasers. In: IPRM 2011; 2011.
[75] Rosales R, Merghem K, Martinez A, Accard A, Lelarge F, Ramdane A. Two-section InAs/InP quantum-dash passively mode locked lasers. In: CLEO: science and innovations; 2011. CThG2.
[76] Asghar H, Wei W, Kumar P, Sooudi E, McInerney JG. Stabilization of self-mode-locked quantum dash lasers by symmetric dual-loop optical feedback. Optics Express 2018;26:4581−92.
[77] Asghar H, Wei W, Kumar P, Sooudi E, Mcinerney JG. Narrow RF linewidth and low timing jitter performance of self-mode-locked quantum dash laser on full delay phase subject to feedback ratio controlled symmetric dual-loop configuration. https://arxiv.org/abs/1708.06612.
[78] Shen A, Gosset C, Renaudier J, Duan G, Oudar J, Lelarge F, et al. Ultra-narrow mode-beating spectral line-width of a passively mode-locked quantum dot Fabry-Perot laser diode. In: Optical communications, 2006. ECOC 2006. European conference on; 2006. p. 1−2.

[79] Shen A, Provost J-G, Akrout A, Rousseau B, Lelarge F, Legouezigou O, et al. Low confinement factor quantum dash (QD) mode-locked Fabry-Perot (FP) laser diode for tunable pulse generation. In: Optical fiber communication conference. OThK1; 2008.
[80] Gosset C, Merghem K, Martinez A, Moreau G, Patriarche G, Aubin G, et al. Subpicosecond pulse generation at 134 GHz and low radiofrequency spectral linewidth in quantum dash-based Fabry-Perot lasers emitting at 1.5 μm. Electronics Letters 2006;42:91−2.
[81] Akrout A, Shen A, Enard A, Duan G-H, Lelarge F, Ramdane A. Low phase noise all-optical oscillator using quantum dash modelocked laser. Electronics Letters 2010;46:73−4.
[82] Latkowski S, Maldonado-Basilio RN, Landais P. Sub-picosecond pulse generation by 40-GHz passively mode-locked quantum-dash 1-mm-long Fabry-PÚrot laser diode. Optics Express 2009;17:19166−72.
[83] Maldonado-Basilio R, Latkowski S, Landais P. 720-fs pulse generation with 40 GHz passively-mode locked quantum-dash Fabry-Perot laser. In: Optical communication, 2009. ECOC '09. 35th European conference on; 2009. p. 1−2.
[84] Maldonado-Basilio R, Parra-Cetina J, Latkowski S, Landais P. Timing-jitter, optical, and mode-beating linewidths analysis on subpicosecond optical pulses generated by a quantum-dash passively mode-locked semiconductor laser. Optics Letters 2010;35:1184−6.
[85] Maldonado-Basilio R, Latkowski S, Surre F, Landais P. Linewidth analysis of 40-GHz passively mode-locked multi-mode semiconductor lasers. Optics Communications 2010;283:299−303.
[86] Latkowski S, Maldonado-Basilio R, Landais P. Short pulse generation with 40 GHz passively-mode locked Q-dashed Fabry-Pérot laser. In: 11th international conference on transparent optical networks, 2009. ICTON '09; 2009. p. 1−4.
[87] Merghem K, Akrout A, Martinez A, Aubin G, Ramdane A, Lelarge F, et al. Pulse generation at 346 GHz using a passively mode locked quantum-dash-based laser at 1.55 μm. Applied Physics Letters 2009;94.
[88] Merghem K, Calò C, Panapakkam V, Martinez A, Lelarge F, Ramdane A. Long-term frequency stabilization of 10-GHz quantum-dash passively mode-locked lasers. IEEE Journal of Selected Topics in Quantum Electronics 2015;21(6):46−52.
[89] Calò C, Schmeckebier H, Merghem K, Rosales R, Lelarge F, Martinez A, et al. Frequency resolved optical gating characterization of sub-ps pulses from single-section InAs/InP quantum dash based mode-locked lasers. Optics Express 2014;22:1742−8.
[90] Calo C, Schmeckebier H, Merghem K, Rosales R, Lelarge F, Martinez A, et al. Frequency-resolved optical gating measurements of sub-ps pulses from InAs/InP quantum dash based mode-locked lasers. In: Indium phosphide and related materials (IPRM), 2013 international conference; 2013. p. 1−2.
[91] Sooudi E, de Dios C, McInerney JG, Huyet H, Lelarge L, Merghem K, et al. A novel scheme for two-level stabilization of semiconductor mode-locked lasers using simultaneous optical injection and optical feedback. IEEE Journal of Selected Topics in Quantum Electronics 2013;19:1101208−11.
[92] Wei W, Asghar H, Kumar P, Marah D, McInerney J. Sub-kHz RF linewidth of quantum-dash mode-locked laser by self-injection from symmetric dual-loop feedback and fiber delay. In: Conference on lasers and electro-optics. OSA Technical Digest; 2016.

[93] Akrout A, Shen A, Brenot R, Dijk FV, Legouezigou O, Pommereau F, et al. Separate error-free transmission of eight channels at 10 Gb/s using comb generation in a quantum-dash-based mode-locked laser. IEEE Photonics Technology Letters 2009; 21(23):1746−8.
[94] Nguyen QT, Besnard P, Bramerie L, Shen A, Kazmierski C, Chanlou P, Duan GH, Simon JC. Bidirectional 2.5-Gb/s WDM-PON using FP-LDs wavelength-locked by a multiple-wavelength seeding source based on a mode-locked laser. IEEE Photonics Technology Letters 2010;22(11):733−5.
[95] Silva MCE, Bramerie L, Gay M, Lobo S, Joindot M, Simon JC. 4×170 Gbit/s DWDM/OTDM transmission using only one quantum dash Fabry Perot mode-locked laser. In: 36th European conference and exhibition on optical communication; 2010. p. 1−3.
[96] M'Sallem YB, Le QT, Bramerie L, Nguyen QT, Borgne E, Besnard P, Shen A, et al. Quantum-dash mode-locked laser as a source for 56-Gb/s DQPSK modulation in WDM multicast applications. IEEE Photonics Technology Letters 2011;23(7):453−5.
[97] Gay M, O'Hare A, Bramerie L, Hao Z, Fresnel S, Peucheret C, Besnard P, Joshi S, Barbet S, Lelarge F. Single quantum dash mode-locked laser as a comb-generator in four-channel 112 Gbit/s WDM transmission. In: OFC 2014; 2014. p. 1−3.
[98] Pfeifle J, Watts R, Shkarban I, Wolf S, Vujicic V, Landais P, Chimot N, et al. Simultaneous phase noise reduction of 30 comb lines from a quantum-dash mode-locked laser diode enabling coherent Tbit/s data transmission. In: 2015 optical fiber communications conference and exhibition (OFC); 2015. p. 1−3.
[99] Pfeifle J, Shkarban I, Wolf S, Kemal JN, Weimann C, Hartmann W, Chimot N, et al. Coherent Terabit communications using a quantum-dash mode-locked laser and self-homodyne detection. In: 2015 optical fiber communications conference and exhibition (OFC); 2015. p. 1−3.
[100] Vujicic V, Calò C, Watts R, Lelarge F, Browning C, Merghem K, Martinez A, Ramdane A, Barry LP. Quantum dash passively mode-locked lasers for Tbit/s data interconnects. In: 2015 optical fiber communications conference and exhibition (OFC); 2015. p. 1−3.
[101] Vujicic V, Calò C, Watts R, Lelarge F, Browning C, Merghem K, Martinez A, Ramdane A, Barry LP. Quantum dash mode-locked lasers for data centre applications. IEEE Journal of Selected Topics in Quantum Electronics November 2015;21(6):53−60.
[102] Kemal JN, Marin-Palomo P, Merghem K, Aubin G, Calo C, Brenot R, Lelarge F, et al. 32QAM WDM transmission using a quantum-dash passively mode-locked laser with resonant feedback. In: 2017 optical fiber communications conference and exhibition (OFC); 2017. p. 1−3.
[103] Rosales R, Charbonnier B, Merghem K, Van Dijk F, Lelarge F, Martinez A, Ramdane A. InAs/InP quantum dash based mode locked lasers for 60 GHz radio over fiber applications. In: 2012 international conference on indium phosphide and related materials; 2012. p. 185−7.
[104] Khan MTA, Alkhazraji E, Ragheb AM, Fathallah H, Alshebeili S, Khan MZM. 100 Gb/s single channel transmission using injection-locked 1621 nm quantum-dash laser. IEEE Photonics Technology Letters 2017;29(6):543−6.
[105] Khan MTA, Shemis MA, Ragheb A, Esmail MA, Fathallah H, Alshebieli S, Khan MZM. 4 m/100 Gb/s optical wireless communication based on far L-band injection locked quantum-dash laser. IEEE Photonics Journal 2017;9(2):1−7.

[106] Shemis MA, Ragheb AM, Khan MTA, Fathallah HA, Alshebeili S, Qureshi KK, Khan MZM. L-band quantum-dash self-injection locked multiwavelength laser source for future WDM access networks. IEEE Photonics Journal 2017;9(5):1−7.

[107] Shemis MA, Ragheb AM, Alkhazraji E, Esmail MA, Fathallah H, Alshebeili S, Alshebeili S, Khan MZM. Self-seeded quantum-dash laser based 5 m−128 Gb/s indoor free-space optical communication. Chinese Optics Letters 2017;15(10):100604.